ACS MATERIALS LETTERS

www.acsmaterialsletters.org

LETTER

Stimulated Emission Depletion (STED) Super-Resolution Imaging with an Advanced Organic Fluorescent Probe: Visualizing the Cellular Lipid Droplets at the Unprecedented Nanoscale Resolution

Ri Zhou, Chenguang Wang,* Xishuang Liang, Fangmeng Liu, Xu Yan, Xiaomin Liu, Peng Sun, Hongyu Zhang, Yue Wang, and Geyu Lu*

Cite This: *ACS Materials Lett.* 2021, 3, 516–524

Read Online

ACCESS | Metrics & More | Article Recommendations | Supporting Information

ABSTRACT: **Lipid droplets (LDs) are important cellular organelles associated with many physiological processes. To visualize and study LDs, particularly the nascent LDs (diameters of 30−60 nm), super-resolution fluorescence imaging techniques with nanoscale resolution are regarded as the most appealing tools. However, this idea is largely limited by the availability of advanced LDs fluorescent probes that are capable of the proper super-resolution imaging techniques. Therefore, visualizations of LDs at the nanoscale resolution are very challenging and highly attractive. Herein, a distyrylbenzene-based molecule Lipi-DSB is sophisticatedly developed as a new LDs fluorescent probe that is capable of the stimulated emission depletion (STED) super-resolution imaging. The probe Lipi-DSB displays superior properties including high photostability and brightness, large Stokes shift, low saturation intensity for STED laser, and good staining specificity toward LDs. Employing this fluorescent probe for STED imaging provides the state-of-the-art super-resolution imaging of LDs in terms of (1) the highest resolution (58 nm) of LDs up to date; (2) the maximum frames (1000 frames, 21.8 min) of time-lapse live imaging of LDs; (3) the first visualization of the fusion process of nascent LDs; (4) and the highest quality of 3D imaging of LDs. Thus, the dynamics and spatial distribution of LDs are visualized at the unprecedented nanoscale resolution, highlighting the utility of this fluorescent probe in STED super-resolution imaging.**

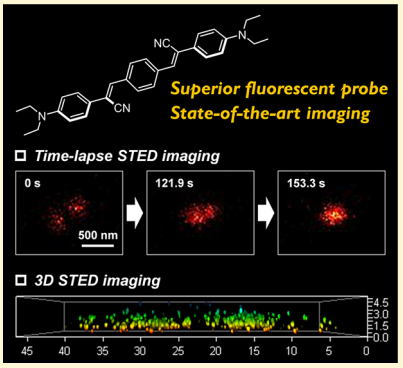

Lipid droplets (LDs) are spherical organelles that consist of a core of neutral lipids such as triglycerides and cholesterol esters, and a surrounding membrane of phospholipid monolayer anchored with proteins. Depending on the cell types, the sizes of LDs range widely.[1,2] For instance, the diameters of LDs are ∼10−200 μm in adipocytes, while only 0.1−1 μm in brown adipose tissue, liver, and heart. Moreover, the diameters are even 30−60 nm for the nascent LDs, which are freshly formed by budding off from the endoplasmic reticulum (ER). Until somewhat recently, LDs were widely regarded as inert fat particles; however, progress in the field has continued to demonstrate their vast roles in a number of cellular processes including membrane trafficking, protein storage, inflammation and so on. Thus, the study of LDs has emerged as one of the most exciting areas of cell biology during the past decade.[1−5]

To visualize LDs and study their versatile functions, the fluorescence imaging techniques (confocal, wide-field, and two-photon microscopies) are generally employed. Accordingly, many organic fluorescent probes have been developed for imaging cellular LDs.[6−16] However, because of the light diffraction, the resolutions of these fluorescence microscopies are inherently limited to be ∼250 nm. Thus, visualizations of the small LDs—particularly, the nascent LDs—are very difficult for these fluorescence imaging techniques. Transmission electron microscopy (TEM) with nanoscale resolution

Received: February 28, 2021
Accepted: April 8, 2021
Published: April 12, 2021

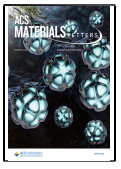

https://doi.org/10.1021/acsmaterialslett.1c00143
ACS Materials Lett. 2021, 3, 516−524

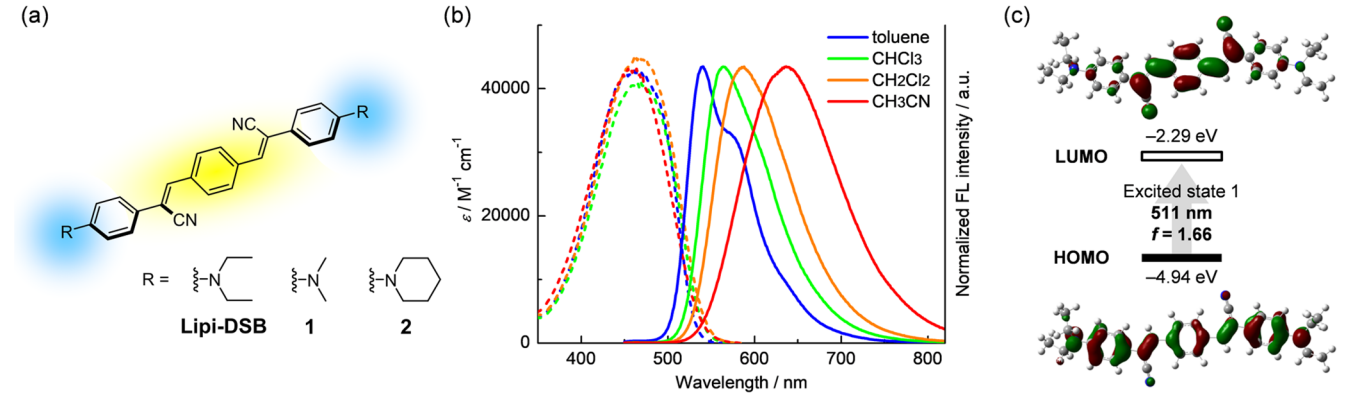

Figure 1. (a) Molecular structures of the fluorescent probe Lipi-DSB and its analogues 1 and 2. (b) Absorption (dashed line) and fluorescence (solid line) spectra of Lipi-DSB in various organic solvents. (c) TD-DFT calculation (B3LYP/6-31G*, Gaussian 09) result of Lipi-DSB: energy diagram, Kohn−Sham HOMO and LUMO, vertical excitation wavelength, and oscillator strengths (f). The first excited state corresponds to the transition of HOMO to LUMO.

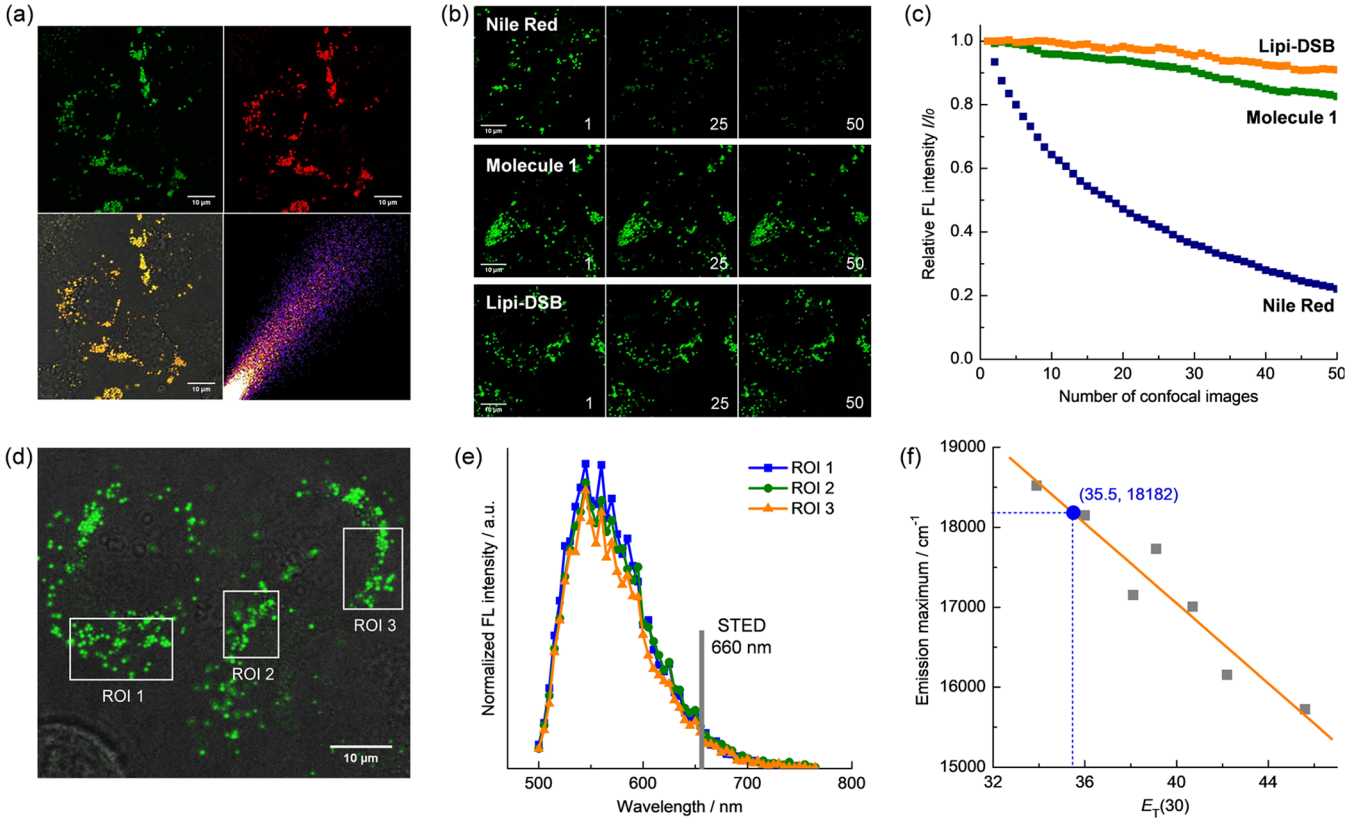

Figure 2. (a) Co-localization confocal imaging of living HeLa cells stained with Lipi-DSB and the lipid droplets probe Ph-Red: green imaging channel of Lipi-DSB; deep red imaging channel of Rh-Red; merged image of two fluorescence channels and bright filed; Pearson's correlation coefficient plot of the two fluorescence channels (R = 0.96); scale bar: 10 μm. (b,c) Comparison of the photostability of Lipi-DSB, molecule 1 and Nile Red on the basis of the repeatedly recording confocal images of HeLa cells in the same area: (b) the confocal images of number 1, 25, and 50; scale bar: 10 μm; (c) the fluorescence intensity of each image (I) relative to the initial value (I_0) plotted as a function of the recorded number. (d,e) The fluorescence spectra of Lipi-DSB in the LDs of living HeLa cells; three regions of interest (ROI) are measured; scale bar: 10 μm. (f) The emission maxima (in wavenumber) of Lipi-DSB as a function of the polarity index $E_T(30)$ of various solvents.

has been employed for this purpose, but it is only capable of analyzing fixed cells and cannot provide the temporal information on LDs in living cells.

In this context, super-resolution imaging techniques have become increasingly important as tools to visualize organelle structures and dynamic processes on the nanoscale.[17,18] Therefore, a few LDs-specific fluorescent probes have been developed very recently for various super-resolution imaging techniques, including structured illumination microscopy (SIM),[19,20] photoactivated localization microscopy (PALM),[21] and stimulated emission depletion microscopy (STED).[22−25] These reports enable the visualization of LDs with a higher resolution than the conventional fluorescence microscopies, demonstrating the utility of these fluorescent

https://doi.org/10.1021/acsmaterialslett.1c00143
ACS Materials Lett. 2021, 3, 516−524

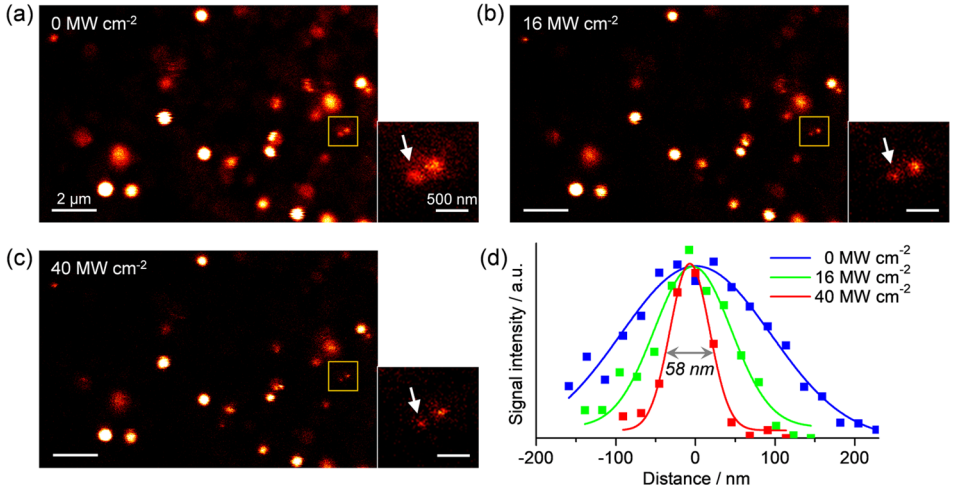

Figure 3. (a–c) Resolution of image dependence on the STED laser power, the STED images of living HeLa cell stained with Lipi-DSB were recorded under excitation at 488 nm and depletion at 660 nm (CW-STED, with laser powers of 0 (panel (a)), 16 (panel (b)), and 40 MW cm^{-2} (panel (c))) (scale bar = 2 μm); the enlarged views of the regions marked with squares are shown in the insets (scale bar = 500 nm), and the images were shown with raw data, without deconvolution. (d) The signal intensity profiles crossed the LDs (indicated by the arrow), the fwhm resolutions were calculated from Gaussian fitting.

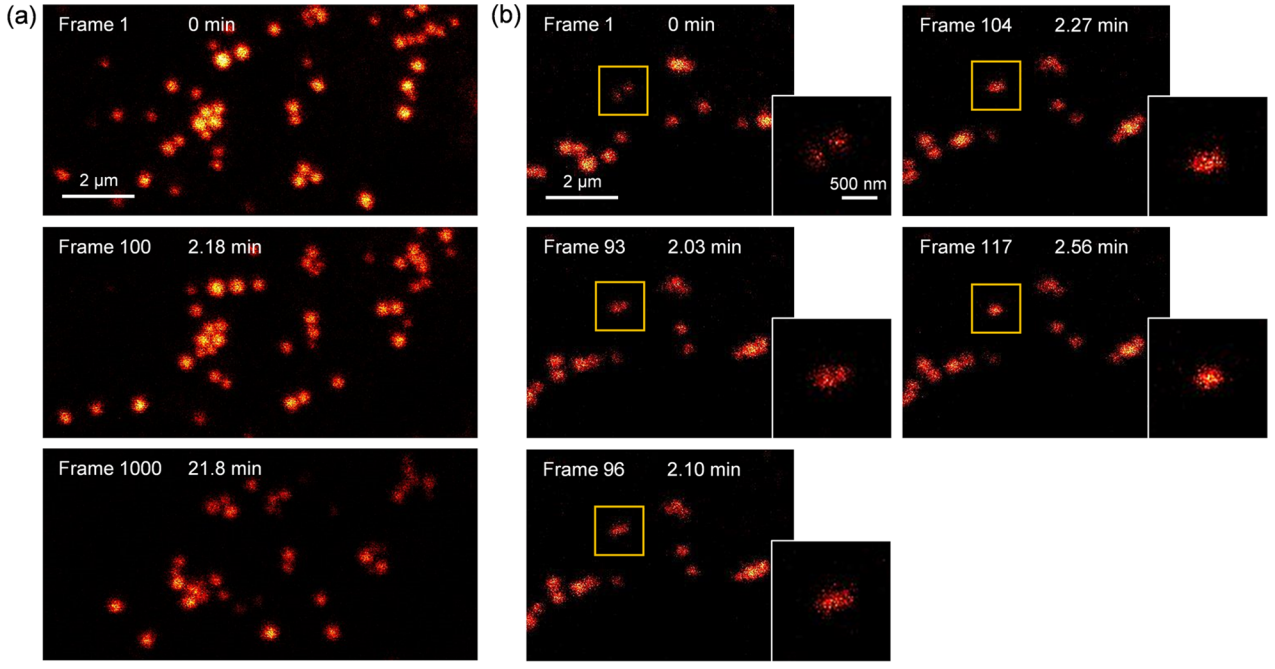

Figure 4. Time-lapse STED super-resolution imaging of living HeLa cells stained with Lipi-DSB. (a) Recording 1000 frames (21.8 min) while maintaining meaningful fluorescence signals (scale bar = 2 μm). (b) The fusion process of two nearby nascent LDs (scale bar = 2 μm); the zoomed views of the square marked regions are shown in the insets (scale bar = 500 nm). The STED images were recorded under excitation at 488 nm and depletion at 660 nm (CW-STED, 40 MW cm^{-2}); the time-lapse STED imaging was shown in raw data without the photobleaching correction or deconvolution.

probes in super-resolution imaging.[19−25] However, these fluorescent probes are still not sufficient to visualize the small LDs particular the nascent LDs, because of the low resolution (see Table S1 in the Supporting Information). Moreover, the photostabilities of these probes are relatively low, which directly limit the multiple acquisitions of super-resolution images, e.g., time-lapse imaging to track the dynamics of LDs and 3D imaging to visualize the spatial distribution of LDs. Therefore, the development of advanced fluorescent probes, which are capable of the proper super-resolution imaging techniques and are able to visualize the cellular LDs and track their dynamics at the unprecedented nanoscale resolution, is highly desired and essential for the biological study of LDs.

Among various super-resolution imaging techniques, we focus on STED microscopy, since it offers the highest spatiotemporal resolution.[26] For STED super-resolution imaging, it inherently requires that (1) the fluorescent probes can be efficiently depleted by the STED laser, which is essential to obtain high resolution; and (2) the fluorescent probes display significantly high photostability, because the STED laser is extremely strong (10−100 MW cm^{-2}).[27,28]

https://doi.org/10.1021/acsmaterialslett.1c00143
ACS Materials Lett. 2021, 3, 516−524

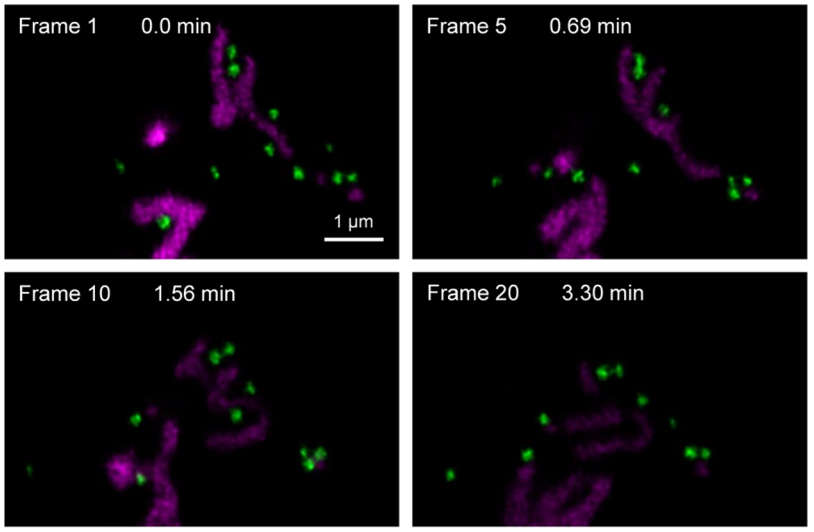

Figure 5. Two-color STED super-resolution imaging of living HeLa cells. The LDs (green pseudo color) and mitochondria (purple pseudo color) were labeled with Lipi-DSB and TMRM, respectively (scale bar = 1 μm); the STED images were recorded under two excitation lasers (470 nm for Lipi-DSB, 550 nm for TMRM) and one STED laser (660 nm CW-STED, 40 MW cm^{-2}). The fluorescence of mitochondria was photobleached quickly due to the insufficient photostability of TMRM.

While the commonly used fluorescent probes do not meet these severe requirements, the development of advanced probes that are capable of STED super-resolution imaging is very challenging and has attracted much attention.[29−42]

Herein, we report a distyrylbenzene-based derivative Lipi-DSB (Figure 1a) as a new LDs fluorescent probe for STED super-resolution imaging. The probe Lipi-DSB displays superior properties, including high photostability and brightness, large Stokes shift, low saturation intensity for STED laser, and good staining specificity toward LDs. Employing the probe for STED imaging of LDs achieved a high resolution of 58 nm, which was substantially below the diffraction limit of light and was the highest resolution of super-resolution imaging of LDs to date. More importantly, the high photostability of the probe enabled state-of-the-art time-lapse STED imaging (up to 1000 frames) to be performed to track the dynamics of LDs in living cells. Thus, the fusion process of nascent LDs was impressively visualized for the first time. In addition, the fluorescent probe was successfully applied in two-color STED imaging to reveal the interactions between LDs and mitochondria in living cells, and was used in 3D STED imaging to visualize the spatial distribution of LDs in fixed cells.

The molecular design of fluorescent probe Lipi-DSB (Figure 1a) is based on the distyrylbenzene skeleton, in which the electron-donating amino groups and the electron-accepting cyano moieties are introduced to the terminals and the center of the molecule, respectively. The thus-obtained donor−acceptor−donor-type molecule displays high brightness while ensuring large Stokes shift. Note that the large Stokes shift not only facilitates the depletion process of fluorescent probe under the STED laser, but also is beneficial to the application in two-color STED imaging (*vide infra*). Moreover, the cyano groups significantly contribute the high photostability of fluorescent probe, while the amino moieties could tune the staining specificity toward LDs. The chemical synthesis and characterization data of the probe Lipi-DSB and its analogues **1** and **2** are shown in Scheme S1 in the Supporting Information.

The photophysical properties of these molecules were studied next (see Figure 1b, as well as Figures S1 and S2 and Table S2 in the Supporting Information). The fluorescent probe Lipi-DSB exhibits an absorption maximum (λ_{abs}) at 460−470 nm, irrespective of the solvent, with molar absorption coefficient (ε) values of ~4.3 × 10^4 M^{-1} cm^{-1}. In contrast, the emission maximum (λ_{em}) of Lipi-DSB is strongly dependent on the solvent polarity, because of the increased dipole moment of molecule in the excited state. As the solvent polarity increases from toluene to CH_3CN, its λ_{em} is shifted from 540 nm to 636 nm. Importantly, Lipi-DSB displays a large Stokes shifts while maintaining high fluorescence quantum yields (Φ_F), e.g., 75 nm and 0.97 in toluene, 119 nm and 0.93 in CH_2Cl_2, and 174 nm and 0.65 in CH_3CN. The fluorescence brightness of Lipi-DSB, as determined by $\varepsilon \times \Phi_F$, is 4.15 × 10^4 M^{-1} cm^{-1} in toluene. This value is significantly higher than that of Nile Red (2.41 × 10^4 M^{-1} cm^{-1} in toluene) which is a representative LDs probe.[6] The emission property of Lipi-DSB was further investigated in aqueous solution, as well as in solid state. In the mixture solution of PBS/DMSO (3/7 (v/v)), Lipi-DSB displays intense red emission (λ_{em} = 623 nm) with a high Φ_F of 0.71 (see Figure S3a in the Supporting Information). In solid state, this probe also exhibits strong red emission (λ_{em} = 641 nm, Φ_F = 0.60), revealing its potential application as a nanoparticle-based fluorescent probe (see Figure S3b in the Supporting Information).

The large Stokes shift and high Φ_F are generally conflicted with each other. To deeply understand the unique fluorescence property of Lipi-DSB, TD-DFT calculation has been conducted (Figure 1c). The highest energy occupied molecular orbital (HOMO) is delocalized over the entire π-skeleton, while the lowest energy unoccupied molecular orbital (LUMO) is mainly located at the central dicyanodistyrylbenzene moiety. The separation between HOMO and LUMO would increase the dipole moment of molecule in the excited state, thus resulting large Stokes shift as well as significant solvatochromism of fluorescence. On the other hand, the donor−acceptor−donor-type distyrylbenzene skeleton maintains a large oscillator strength of 1.66 between the transition of HOMO → LUMO. Thus, radiative process from the first excited state (S1) to the ground state (S0) should be very

https://doi.org/10.1021/acsmaterialslett.1c00143
ACS Materials Lett. 2021, 3, 516−524

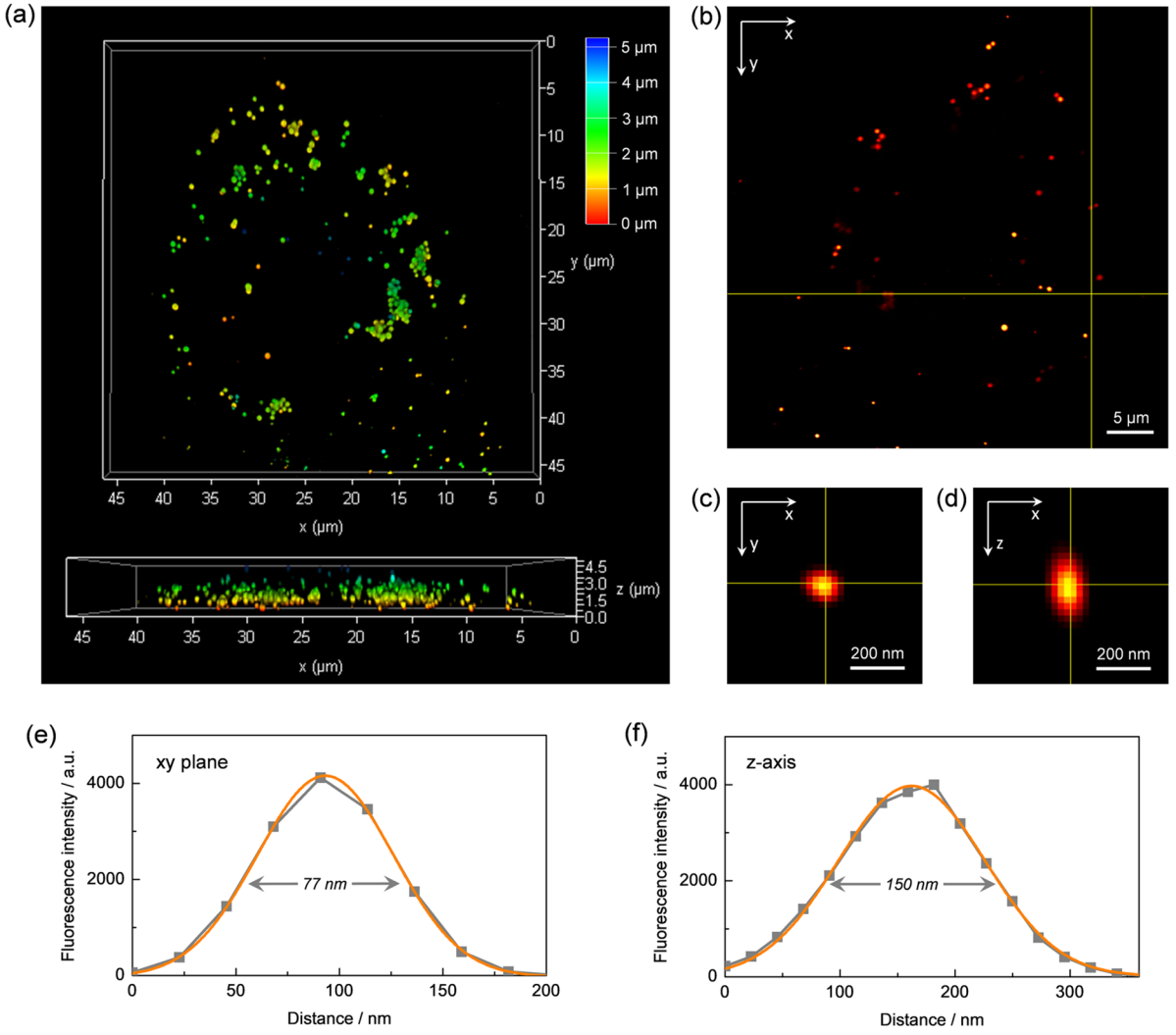

Figure 6. 3D STED super-resolution imaging of the fixed HeLa cells stained with LDs fluorescent probe Lipi-DSB. (a) Top view and side view of the 3D STED image; the variation of color from blue to red denotes the different *z*-depths. (b–d) Orthogonal view (*xy* and *xz* planes) of a small lipid droplet, which was used for determination of the fwhm resolution. (e, f) The signal intensity profile (gray line) crossed the lipid droplet; the fwhm resolutions of the *xy* plane and *z*-axis were calculated from Gaussian fitting (orange line).

reasonable, and a high Φ_F can be expected. This speculation has also been experimentally supported by the relatively large value of the radiative decay rate constant (see Table S2 in the Supporting Information).

We then investigated the cell-staining properties of probe Lipi-DSB and its analogues **1** and **2**. In consideration of the absorption and emission properties, the co-staining experiments of these molecules were paired with Ph-Red, which is a nice LDs fluorescent probe with high specificity.[16] The two imaging channels of Lipi-DSB and Ph-Red indeed did not cross-talk with each other (see Figure S4 in the Supporting Information). The live HeLa cells were incubated with Lipi-DSB (2 μM) and Ph-Red (500 nM) for 2 h. As shown in Figure 2a, the two imaging channels displayed good co-localization, with a Pearson's correlation coefficient (R) value of 0.96, which indicates the high LDs specificity of Lipi-DSB. The co-staining experiments of molecules **1** and **2** were also conducted (see Figures S5 and S6 in the Supporting Information). It was revealed that the LDs specificity of molecule **1** (R = 0.96) is high, while that of molecule **2** is moderate (R = 0.70). In addition, the co-staining experiment of Lipi-DSB and a commercially available lysosome probe LysoTracker Deep Red directly excluded the lysosome-targeting possibility of this LDs probe (see Figure S7 in the Supporting Information).

The high LDs specificities of probe Lipi-DSB and molecule **1** were further demonstrated by the analysis of signal intensity profiles across the LDs (see Figure S8 in the Supporting Information). The signal-to-noise ratios of probe Lipi-DSB and molecule **1** are substantially higher than those of molecule **2** and the representative LDs probe Nile Red. Indeed, the nonspecific staining of molecule **2** and Nile Red could be observed. The comparison of Lipi-DSB and its analogues **1** and **2** demonstrates that the terminal amino groups of these molecules display an important role in the tuning of the staining specificity toward LDs.

Moreover, the photostability of probe Lipi-DSB was evaluated and compared with those of molecule **1** and Nile Red. Under the identical and intense excitation condition (λ_{ex} = 488 nm), the confocal images of LDs stained with these probes were recorded repeatedly in the same area (Figure 2b). While Nile Red was photobleached very quickly during imaging, Lipi-DSB and molecule **1** displayed much higher photostability. After recording 50 confocal images, Lipi-DSB

https://doi.org/10.1021/acsmaterialslett.1c00143
ACS Materials Lett. 2021, 3, 516–524

and molecule **1** maintained 91% and 83% of their initial fluorescence signals, which were significantly higher than that of Nile Red (22%) (Figure 2c). The high photostability of Lipi-DSB should be strongly related with the two strong electron-withdrawing cyano groups, which largely decrease the HOMO/LUMO levels as well as significantly protect the C=C double bonds. In consideration of the fact that Nile Red is already photostable enough for recording several frames of STED imaging, Lipi-DSB, which exhibits much improved photostability, is therefore expected to be capable of time-lapse STED imaging and 3D STED imaging consisting of much more frames.

The cytotoxicity of Lipi-DSB was also evaluated by MTT assay (see Figure S9 in the Supporting Information). With a concentration up to 10 μM, the probe did not affect the cell viability within 24 h. Based on the MTT data, the IC50 value of Lipi-DSB has been calculated to be 14.7 μM by using the SPSS Statistics software. The relatively high value of IC50 further reveals the good biocompatibility of Lipi-DSB. Generally, staining cells with Lipi-DSB in a concentration of 0.5−2 μM for 2 h could provide sufficient fluorescence brightness for confocal and STED imaging. All these results demonstrate the outstanding utility of Lipi-DSB for LDs staining.

Moreover, the fluorescence property of Lipi-DSB in cellular LDs was studied by in situ lambda scan. Three different regions of living HeLa cells were measured, providing similar emission spectra with λ_{em} of 550 nm (see Figures 2d and 2e). Since the absorption of Lipi-DSB is not sensitive to the environment, the Stokes shift of probe in LDs should be ∼80 nm. This Stokes shift value is relatively large and is highly desired for STED imaging (*vide infra*). The in situ measurements of emission spectra of Lipi-DSB also enabled to determine the polarity of LDs in living cells. For this purpose, the emission maxima (in wavenumber) of Lipi-DSB in various solvents are plotted as a function of the polarity index $E_T(30)$ (see Figure 2f, as well as Figure S10 and Table S3 in the Supporting Information).[43,44] Based on the linear fitting of them, the emission maximum of Lipi-DSB in LDs (18 349 cm^{-1}) is calculated to correspond to a $E_T(30)$ value of 35.2. This value is comparable to those of toluene and dioxane, indicating a very hydrophobic nature of LDs.

The characteristic features of Lipi-DSB, including its high photostability and brightness, large Stokes shift, and good staining specificity toward LDs, suggested its promising utility for STED super-resolution imaging. Initially, we investigated the depletion efficiency of Lipi-DSB under the continuous wave STED laser (Leica TCS SP8 STED system, CW-STED, 660 nm). The 592 nm CW-STED laser was not employed because this laser would directly excite Lipi-DSB. The living HeLa cells stained with the probe were imaged under the identical excitation condition (λ_{ex} = 488 nm) while gradually increasing the STED laser power (see Figure S11a in the Supporting Information). Consequently, the fluorescence signals were significantly depleted by the STED laser. Based on the plotting of the fluorescence intensities of each image as a function of the STED laser intensities, the saturation intensity (I_{sat}) of Lipi-DSB, at which half of fluorescence intensity will be depleted, is determined to be 10.1 MW cm^{-2} (see Figure S11b in the Supporting Information). This I_{sat} value is comparable or even lower than that of the golden standard STED imaging probe ATTO 647N (10−20 MW cm^{-2}),[31,45,46] demonstrating the superior depletion efficiency of Lipi-DSB. This result should be due to that the large Stokes shift of Lipi-DSB enables the STED laser to have significant overlap with the emission spectrum, while being far away from the absorption band avoiding the re-excitation.

The STED laser power-dependent resolution then was studied. The images of living HeLa cells stained with Lipi-DSB were recorded under the STED laser powers of 0, 16, and 40 MW cm^{-2}, respectively. As the STED power increases, the images of LDs become sharper and sharper (see Figures 3a−c). Accordingly, the full width at half maxima (fwhm) resolutions of images are largely improved from 222 ± 21 nm under a laser power of 0 MW cm^{-2} to 118 ± 14 nm under a laser power of 16 MW cm^{-2}, and further to 58 ± 4 nm under a laser power of 40 MW cm^{-2} (Figure 3d). The resolution of 58 nm is substantially below the diffraction limit of light and represents the highest resolution of super-resolution imaging of LDs to date (see Table S1 in the Supporting Information).[19−25] Further improvement in the resolution to better than 58 nm may be achieved by designing the fluorescent probes with lower saturation intensity and combining with the time-gated detection method. It is proposed that Lipi-DSB is located at the core or both core and outer membrane of LDs. However, if the probe is located at the outer membrane, the LDs would be visualized as donut rings under STED imaging.

Importantly, the high photostability of Lipi-DSB enabled us to conduct time-lapse STED imaging to track the dynamics of LDs in living cells. Under a strong STED power of 40 MW cm^{-2}, the time-lapse STED imaging with a high resolution of 57 ± 6 nm was successfully recorded up to 1000 frames (21.8 min, 0.763 fps) while maintaining meaningful fluorescence signals (see Figure 4a, as well as Figure S12 and Movie S1 in the Supporting Information). During the STED imaging, the lipid droplets are continuously moving as usual within 21.8 min. Further extending to longer time, the living cells sometimes would be significantly shrunken, reflecting the photodamage caused by the STED laser. This is a very impressive result, since the strong STED laser generally causes serious photobleaching of fluorescent probes, even the recently reported highly photostable ones still encounter this problem and are only capable of recording tens or hundreds of frames in time-lapse STED imaging (see Table S4 in the Supporting Information).[29−35] The probe Lipi-DSB displaying a state-of-the-art performance of time-lapse STED imaging is thus highly desired for studying the dynamics of LDs in living cells on the nanoscale.

The nascent LDs, of which the sizes are only ∼30−60 nm, are freshly formed by budding off from the endoplasmic reticulum. As the newly generated organelles, the nascent LDs are highly active and had a tendency to fuse with each other or fuse with larger LDs. The fusion is one of the important ways in which nascent lipid droplets would mature and grow. Visualization of the dynamics of nascent LDs is critical to reveal their biological functions. However, because of the insufficient resolution, the conventional fluorescence imaging techniques cannot be used for this purpose. The electron microscopy with high resolution is also not suitable, because only fixed cells can be measured. The fluorescent probe Lipi-DSB, which is capable of long-term time-lapse STED imaging with nanoscale resolution, provides an important opportunity for tracking the dynamics of nascent LDs. Indeed, the fusion process of two nascent LDs of which the distance between them was ∼350 nm, was impressively visualized by time-lapse STED imaging (see Figure 4b, as well as Movie S2 in the

https://doi.org/10.1021/acsmaterialslett.1c00143
ACS Materials Lett. 2021, 3, 516−524

Supporting Information). Two nascent LDs were gradually approached with each other and fused together, generating a larger LD in 2.5 min. To the best of our knowledge, this is the first report to uncover the fusion process of nascent LDs, highlighting the utility of the fluorescent probe.

Moreover, the large Stokes shift of probe Lipi-DSB facilitates its application in two-color STED imaging, which is a powerful tool to study the interactions between two different organelles on the nanoscale.[47] Tetramethylrhodamine methyl ester (TMRM), which is a mitochondria fluorescent probe with a small Stokes shift, was paired with Lipi-DSB for this two-color experiment. Because of the significant difference in the Stokes shift, Lipi-DSB and TMRM can be selectively excited by two lasers (470 and 550 nm), while efficiently depleted by the identical STED laser (660 nm) (see Figure S13 in the Supporting Information). In addition, the two-color STED images were acquired via a line-by-line sequential scanning of two channels with one detector (λ_{em} = 560−640 nm) to suppress the positional deviation of two images caused by rapid movements of LDs and mitochondria in living cells. As shown in Figure 5, as well as Figure S14 in the Supporting Information, the dynamics of LDs and mitochondria were successfully monitored in 3.30 min by time-lapse two-color STED imaging consisting of 20 frames. Further extending the period of time-lapse imaging was limited by the insufficient photostability of TMRM. This result not only demonstrates the utility of Lipi-DSB in two-color STED imaging as a LDs-specificity fluorescent probe, but also proves its high photostability, since both Lipi-DSB and TMRM are irradiated by the identical intense STED laser.

Finally, the probe Lipi-DSB was applied in 3D STED imaging to visualize the spatial distribution of LDs in fixed cells. Generally, the 3D STED image is obtained by reconstruction of Z-stack STED slices, which involve multiple imaging scans of the sample and lead to very serious photobleaching of the fluorescent probe.[33,48] Consequently, the 3D STED imaging is a very challenging task, similar to the time-lapse STED imaging. Thanks to the high photostability as well as good retention ability in cells after chemical fixing, Lipi-DSB enables the successful realization of the 3D STED imaging of LDs with high resolution. For this experiment, the live HeLa cells prestained with probe Lipi-DSB were fixed by 4% paraformaldehyde. In order to get high spatial resolution of the three-dimensional (3D) image, the Z-stack STED slices were recorded under a quite precise condition: a strong STED laser power of 40 MW cm^{-2}, a high *xy* pixel resolution of 22.7 nm, and a small *z*-step of 50 nm. Based on the 105 STED slices in a *z*-depth of 5.20 μm, the 3D STED image was successfully reconstructed with high quality (see Figure 6, as well as Movie S3 in the Supporting Information). The spatial distribution of LDs can be precisely visualized. The fwhm resolution of the 3D STED image is 77 ± 1 nm in the *xy* plane and 150 ± 3 nm along the *z*-axis, which is substantially below the diffraction limit of light (~250 nm in the *xy* plane, ~500 nm along the *z*-axis) and is comparable or even better than the recently reported 3D STED imaging of mitochondria and tubulins (see Table S4 in the Supporting Information),[31,33] demonstrating the highest quality of 3D super-resolution imaging of LDs so far (recall Table S1).[23]

In summary, we have developed a new organic fluorescent probe Lipi-DSB that exhibits high photostability and brightness, a large Stokes shift, a low saturation intensity for STED laser, and good staining specificity toward LDs. These features enable the probe to be ideally applied in STED super-resolution imaging of cellular LDs including time-lapse STED imaging and two-color STED imaging, as well as 3D STED imaging. Consequently, the dynamics and the spatial distribution of LDs have been precisely visualized at the unprecedented nanoscale resolution. Moreover, employing the probe for long-term time-lapse STED imaging uncovered the fusion process of nascent LDs for the first time. These results reveal that the fluorescent probe Lipi-DSB could provide a new horizon for the biological study of LDs.

■ ASSOCIATED CONTENT

Supporting Information

The Supporting Information is available free of charge at https://pubs.acs.org/doi/10.1021/acsmaterialslett.1c00143.

Chemical synthesis and characterization data of all new compounds, photophysical data for **1** and **2**, additional fluorescence imaging data, and MTT assay results (PDF)

Time-lapse STED imaging (1000 frames) (Movie S1) (AVI)

The fusion process of nascent LDs (Movie S2) (AVI)

3D STED imaging of LDs (Movie S3) (AVI)

■ AUTHOR INFORMATION

Corresponding Authors

Chenguang Wang − *State Key Laboratory on Integrated Optoelectronics, Key Laboratory of Advanced Gas Sensors of Jilin Province, College of Electronic Science & Engineering, Jilin University, Changchun 130012, China;* orcid.org/0000-0001-9770-1062; Email: wangchenguang@jlu.edu.cn

Geyu Lu − *State Key Laboratory on Integrated Optoelectronics, Key Laboratory of Advanced Gas Sensors of Jilin Province, College of Electronic Science & Engineering, Jilin University, Changchun 130012, China;* orcid.org/0000-0002-7428-2456; Email: lugy@jlu.edu.cn

Authors

Ri Zhou − *State Key Laboratory on Integrated Optoelectronics, Key Laboratory of Advanced Gas Sensors of Jilin Province, College of Electronic Science & Engineering, Jilin University, Changchun 130012, China*

Xishuang Liang − *State Key Laboratory on Integrated Optoelectronics, Key Laboratory of Advanced Gas Sensors of Jilin Province, College of Electronic Science & Engineering, Jilin University, Changchun 130012, China*

Fangmeng Liu − *State Key Laboratory on Integrated Optoelectronics, Key Laboratory of Advanced Gas Sensors of Jilin Province, College of Electronic Science & Engineering, Jilin University, Changchun 130012, China*

Xu Yan − *State Key Laboratory on Integrated Optoelectronics, Key Laboratory of Advanced Gas Sensors of Jilin Province, College of Electronic Science & Engineering, Jilin University, Changchun 130012, China;* orcid.org/0000-0003-2152-675X

Xiaomin Liu − *State Key Laboratory on Integrated Optoelectronics, Key Laboratory of Advanced Gas Sensors of Jilin Province, College of Electronic Science & Engineering, Jilin University, Changchun 130012, China;* orcid.org/0000-0003-4186-9637

https://doi.org/10.1021/acsmaterialslett.1c00143
ACS Materials Lett. 2021, 3, 516−524

Peng Sun − *State Key Laboratory on Integrated Optoelectronics, Key Laboratory of Advanced Gas Sensors of Jilin Province, College of Electronic Science & Engineering, Jilin University, Changchun 130012, China;* orcid.org/0000-0002-9509-9431

Hongyu Zhang − *State Key Laboratory of Supramolecular Structure and Materials, College of Chemistry, Jilin University, Changchun 130012, China;* orcid.org/0000-0002-0219-3948

Yue Wang − *State Key Laboratory of Supramolecular Structure and Materials, College of Chemistry, Jilin University, Changchun 130012, China;* orcid.org/0000-0001-6936-5081

Complete contact information is available at: https://pubs.acs.org/10.1021/acsmaterialslett.1c00143

Notes

The authors declare no competing financial interest.

■ ACKNOWLEDGMENTS

This work is supported by the National Nature Science Foundation of China (Nos. 61831011, 61833006, 62075079, and 61875191).

■ REFERENCES

(1) Olzmann, J. A.; Carvalho, P. Dynamics and functions of lipid droplets. *Nat. Rev. Mol. Cell Biol.* **2019**, *20*, 137−155.

(2) Thiam, A. R.; Beller, M. The why, when and how of lipid droplet diversity. *J. Cell Sci.* **2017**, *130*, 315−324.

(3) Thiam, A. R.; Farese, R. V., Jr.; Walther, T. C. The biophysics and cell biology of lipid droplets. *Nat. Rev. Mol. Cell Biol.* **2013**, *14*, 775−786.

(4) Walther, T. C.; Farese, R. V., Jr. Lipid Droplets and Cellular Lipid Metabolism. *Annu. Rev. Biochem.* **2012**, *81*, 687−714.

(5) Farese, R. V., Jr.; Walther, T. C. Lipid Droplets Finally Get a Little R-E-S-P-E-C-T. *Cell* **2009**, *139*, 855−860.

(6) Fam, T. K.; Klymchenko, A. S.; Collot, M. Recent Advances in Fluorescent Probes for Lipid Droplets. *Materials* **2018**, *11* (9), 1768.

(7) Collot, M.; Fam, T. K.; Ashokkumar, P.; Faklaris, O.; Galli, T.; Danglot, L.; Klymchenko, A. S. Ultrabright and Fluorogenic Probes for Multicolor Imaging and Tracking of Lipid Droplets in Cells and Tissues. *J. Am. Chem. Soc.* **2018**, *140*, 5401−5411.

(8) Collot, M.; Bou, S.; Fam, T. K.; Richert, L.; Mély, Y.; Danglot, L.; Klymchenko, A. S. Probing Polarity and Heterogeneity of Lipid Droplets in Live Cells Using a Push-Pull Fluorophore. *Anal. Chem.* **2019**, *91*, 1928−1935.

(9) Tatenaka, Y.; Kato, H.; Ishiyama, M.; Sasamoto, K.; Shiga, M.; Nishitoh, H.; Ueno, Y. Monitoring Lipid Droplet Dynamics in Living Cells by Using Fluorescent Probes. *Biochemistry* **2019**, *58*, 499−503.

(10) Shi, L.; Li, K.; Li, L. L.; Chen, S. Y.; Li, M. Y.; Zhou, Q.; Wang, N.; Yu, X. Q. Novel easily available purine-based AIEgens with colour tunability and applications in lipid droplet imaging. *Chem. Sci.* **2018**, *9*, 8969−8974.

(11) Jiang, M. J.; Gu, X. G.; Lam, J. W. Y.; Zhang, Y.; Kwok, R. T. K.; Wong, K. S.; Tang, B. Z. Two-photon AIE bio-probe with large Stokes shift for specific imaging of lipid droplets. *Chem. Sci.* **2017**, *8*, 5440−5446.

(12) Wang, D.; Su, H. F.; Kwok, R. T. K.; Shan, G.; Leung, A. C. S.; Lee, M. M. S.; Sung, H. H. Y.; Williams, I. D.; Lam, J. W. Y.; Tang, B. Z. Facile Synthesis of Red/NIR AIE Luminogens with Simple Structures, Bright Emissions, and High Photostabilities, and Their Applications for Specific Imaging of Lipid Droplets and Image-Guided Photodynamic Therapy. *Adv. Funct. Mater.* **2017**, *27*, 1704039.

(13) Gao, M.; Su, H. F.; Lin, Y. H.; Ling, X.; Li, S.; Qin, A.; Tang, B. Z. Photoactivatable aggregation-induced emission probes for lipid droplets-specific live cell imaging. *Chem. Sci.* **2017**, *8*, 1763−1768.

(14) Gao, M.; Su, H. F.; Li, S. W.; Lin, Y.; Ling, X.; Qin, A.; Tang, B. Z. An easily accessible aggregation-induced emission probe for lipid droplet-specific imaging and movement tracking. *Chem. Commun.* **2017**, *53*, 921−924.

(15) Yamaguchi, E.; Wang, C. G.; Fukazawa, A.; Taki, M.; Sato, Y.; Sasaki, T.; Ueda, M.; Sasaki, N.; Higashiyama, T.; Yamaguchi, S. Environment-Sensitive Fluorescent Probe: A Benzophosphole Oxide with an Electron-Donating Substituent. *Angew. Chem., Int. Ed.* **2015**, *54*, 4539−4543.

(16) Zhou, R.; Cui, Y. Y.; Dai, J. N.; Wang, C. G.; Liang, X. S.; Yan, X.; Liu, F. M.; Liu, X. M.; Sun, P.; Zhang, H. Y.; Wang, Y.; Lu, G. Y. A Red-Emissive Fluorescent Probe with a Compact Single-Benzene-Based Skeleton for Cell Imaging of Lipid Droplets. *Adv. Opt. Mater.* **2020**, *8*, 1902123.

(17) Sahl, S. J.; Hell, S. W.; Jakobs, S. Fluorescence nanoscopy in cell biology. *Nat. Rev. Mol. Cell Biol.* **2017**, *18*, 685−701.

(18) Sigal, Y. M.; Zhou, R. B.; Zhuang, X. W. Visualizing and discovering cellular structures with super-resolution microscopy. *Science* **2018**, *361*, 880−887.

(19) Zheng, X. J.; Zhu, W. C.; Ni, F.; Ai, H.; Yang, C. L. A specific bioprobe for super-resolution fluorescence imaging of lipid droplets. *Sens. Actuators, B* **2018**, *255*, 3148−3154.

(20) Zheng, X. J.; Zhu, W. C.; Ni, F.; Ai, H.; Gong, S.; Zhou, X.; Sessler, J. L.; Yang, C. L. Simultaneous dual-colour tracking lipid droplets and lysosomes dynamics using a fluorescent probe. *Chem. Sci.* **2019**, *10*, 2342−2348.

(21) Tang, J.; Robichaux, M. A.; Wu, K. L.; Pei, J.; Nguyen, N. T.; Zhou, Y.; Wensel, T. G.; Xiao, H. Single-Atom Fluorescence Switch: A General Approach toward Visible-Light-Activated Dyes for Biological Imaging. *J. Am. Chem. Soc.* **2019**, *141*, 14699−14706.

(22) O'Connor, D.; Byrne, A.; Berselli, G. B.; Long, C.; Keyes, T. E. Mega-stokes pyrene ceramide conjugates for STED imaging of lipid droplets in live cells. *Analyst* **2019**, *144*, 1608−1621.

(23) Xu, H. K.; Zhang, H. H.; Liu, G.; Kong, L.; Zhu, X.; Tian, X.; Zhang, Z.; Zhang, R.; Wu, Z.; Tian, Y.; Zhou, H. Coumarin-Based Fluorescent Probes for Super-resolution and Dynamic Tracking of Lipid Droplets. *Anal. Chem.* **2019**, *91*, 977−982.

(24) Taki, M.; Kajiwara, K.; Yamaguchi, E.; Sato, Y.; Yamaguchi, S. Fused Thiophene-S,S-dioxide-Based Super-Photostable Fluorescent Marker for Lipid Droplets. *ACS Materials Lett.* **2021**, *3*, 42−49.

(25) Xu, Y. Z.; Zhang, H. K.; Zhang, N.; Xu, R.; Wang, Z.; Zhou, Y.; Shen, Q.; Dang, D.; Meng, L.; Tang, B. Z. An easily-synthesized AIE luminogen for lipid droplets-specific super-resolution imaging and two-photon imaging. *Mater. Chem. Front.* **2021**, *5*, 1872.

(26) Vicidomini, G.; Bianchini, P.; Diaspro, A. STED super-resolved microscopy. *Nat. Methods* **2018**, *15*, 173−182.

(27) Wang, L.; Frei, M. S.; Salim, A.; Johnsson, K. Small-Molecule Fluorescent Probes for Live-Cell Super-Resolution Microscopy. *J. Am. Chem. Soc.* **2019**, *141*, 2770−2781.

(28) Liu, Z. H.; Liu, J.; Wang, X. D.; Mi, F.; Wang, D.; Wu, C. F. Fluorescent Bioconjugates for Super-Resolution Optical Nanoscopy. *Bioconjugate Chem.* **2020**, *31*, 1857−1872.

(29) Wang, C. G.; Taki, M.; Sato, Y.; Tamura, Y.; Yaginuma, H.; Okada, Y.; Yamaguchi, S. A photostable fluorescent marker for the superresolution live imaging of the dynamic structure of the mitochondrial cristae. *Proc. Natl. Acad. Sci. U. S. A.* **2019**, *116*, 15817−15822.

(30) Stephan, T.; Roesch, A.; Riedel, D.; Jakobs, S. Live-cell STED nanoscopy of mitochondrial cristae. *Sci. Rep.* **2019**, *9*, 12419.

(31) Yang, X. S.; Yang, Z. G.; Wu, Z. Y.; He, Y.; Shan, C.; Chai, P.; Ma, C.; Tian, M.; Teng, J.; Jin, D.; Yan, W.; Das, P.; Qu, J.; Xi, P. Mitochondrial dynamics quantitatively revealed by STED nanoscopy with an enhanced squaraine variant probe. *Nat. Commun.* **2020**, *11*, 3699.

(32) Lukinavičius, G.; Reymond, L.; D'Este, E.; Masharina, A.; Göttfert, F.; Ta, H.; Güther, A.; Fournier, M.; Rizzo, S.; Waldmann, H.; Blaukopf, C.; Sommer, C.; Gerlich, D. W.; Arndt, H. D.; Hell, S. W.; Johnsson, K. Fluorogenic probes for live-cell imaging of the cytoskeleton. *Nat. Methods* **2014**, *11*, 731−733.

(33) Wang, C. G.; Taki, M.; Sato, Y.; Fukazawa, A.; Higashiyama, T.; Yamaguchi, S. Super-Photostable Phosphole-Based Dye for Multiple-Acquisition Stimulated Emission Depletion Imaging. *J. Am. Chem. Soc.* **2017**, *139*, 10374−10381.
(34) Lukinavičius, G.; Blaukopf, C.; Pershagen, E.; Schena, A.; Reymond, L.; Derivery, E.; Gonzalez-Gaitan, M.; D'Este, E.; Hell, S. W.; Gerlich, D. W.; Johnsson, K. SiR-Hoechst is a far-red DNA stain for live-cell nanoscopy. *Nat. Commun.* **2015**, *6*, 8497.
(35) Wang, C. G.; Taki, M.; Kajiwara, K.; Wang, J.; Yamaguchi, S. Phosphole-Oxide-Based Fluorescent Probe for Super-resolution Stimulated Emission Depletion Live Imaging of the Lysosome Membrane. *ACS Materials Lett.* **2020**, *2*, 705−711.
(36) Fang, X. F.; Chen, X. Z.; Li, R. Q.; Liu, Z.; Chen, H.; Sun, Z.; Ju, B.; Liu, Y.; Zhang, S. X. A.; Ding, D.; Sun, Y.; Wu, C. Multicolor Photo-Crosslinkable AIEgens toward Compact Nanodots for Subcellular Imaging and STED Nanoscopy. *Small* **2017**, *13*, 1702128.
(37) Wang, L.; Tran, M.; D'Este, E.; Roberti, J.; Koch, B.; Xue, L.; Johnsson, K. A general strategy to develop cell permeable and fluorogenic probes for multicolour nanoscopy. *Nat. Chem.* **2020**, *12*, 165−172.
(38) Bottanelli, F.; Kromann, E. B.; Allgeyer, E. S.; Erdmann, R. S.; Wood Baguley, S.; Sirinakis, G.; Schepartz, A.; Baddeley, D.; Toomre, D. K.; Rothman, J. E.; Bewersdorf, J. Two-colour live-cell nanoscale imaging of intracellular targets. *Nat. Commun.* **2016**, *7*, 10778.
(39) Spahn, C.; Hurter, F.; Glaesmann, M.; Karathanasis, C.; Lampe, M.; Heilemann, M. Protein-Specific, Multicolor and 3D STED Imaging in Cells with DNA-Labeled Antibodies. *Angew. Chem., Int. Ed.* **2019**, *58*, 18835−18838.
(40) Spahn, C.; Grimm, J. B.; Lavis, L. D.; Lampe, M.; Heilemann, M. Whole-Cell, 3D, and Multicolor STED Imaging with Exchangeable Fluorophores. *Nano Lett.* **2019**, *19*, 500−505.
(41) Gao, Z. S.; Wang, J. H.; Song, P.; Kang, B.; Xu, J. J.; Chen, H. Y. Spaser Nanoparticles for Ultranarrow Bandwidth STED Super-Resolution Imaging. *Adv. Mater.* **2020**, *32*, 1907233.
(42) Li, D. Y.; Qin, W.; Xu, B.; Qian, J.; Tang, B. Z. AIE Nanoparticles with High Stimulated Emission Depletion Efficiency and Photobleaching Resistance for Long-Term Super-Resolution Bioimaging. *Adv. Mater.* **2017**, *29*, 1703643.
(43) Kucherak, O. A.; Didier, P.; Mély, Y.; Klymchenko, A. S. Fluorene Analogues of Prodan with Superior Fluorescence Brightness and Solvatochromism. *J. Phys. Chem. Lett.* **2010**, *1*, 616−620.
(44) Kucherak, O. A.; Richert, L.; Mély, Y.; Klymchenko, A. S. Dipolar 3-methoxychromones as bright and highly solvatochromic fluorescent dyes. *Phys. Chem. Chem. Phys.* **2012**, *14*, 2292−2300.
(45) Liu, Y. J.; Ding, Y. C.; Alonas, E.; Zhao, W.; Santangelo, P. J.; Jin, D.; Piper, J. A.; Teng, J.; Ren, Q.; Xi, P. Achieving $\lambda/10$ resolution CW STED nanoscopy with a Ti:Sapphire oscillator. *PLoS One* **2012**, *7*, No. e40003.
(46) Bianchini, P.; Harke, B.; Galiani, S.; Vicidomini, G.; Diaspro, A. Single-wavelength two-photon excitation-stimulated emission depletion (SW2PE-STED) superresolution imaging. *Proc. Natl. Acad. Sci. U. S. A.* **2012**, *109*, 6390−6393.
(47) Sednev, M. V.; Belov, V. N.; Hell, S. W. Fluorescent dyes with large Stokes shifts for super-resolution optical microscopy of biological objects: A review. *Methods Appl. Fluoresc.* **2015**, *3*, 042004.
(48) Wildanger, D.; Medda, R.; Kastrup, L.; Hell, S. W. A compact STED microscope providing 3D nanoscale resolution. *J. Microsc.* **2009**, *236*, 35−43.

https://doi.org/10.1021/acsmaterialslett.1c00143
ACS Materials Lett. 2021, 3, 516−524